Journal of Materials Chemistry A

A Redox-Active Organic Cation for Safer High Energy Density Li-Ion Batteries

Journal:	*Journal of Materials Chemistry A*
Manuscript ID	TA-ART-06-2020-006133.R1
Article Type:	Paper
Date Submitted by the Author:	20-Jul-2020

Complete List of Authors:	Ji, Weixiao; University of Wisconsin Milwaukee College of Engineering and Applied Science, Mechanical Engineering Huang, He; Cornell University, Chemistry Huang, Xingkang; University of Wisconsin Milwaukee College of Engineering and Applied Science, Mechanical Engineering Zhang, Xiaoxiao; University of Wisconsin Milwaukee College of Engineering and Applied Science, Mechancial Zheng, Dong; University of Wisconsin Milwaukee, Mechanical Engineering Ding, Tianyao; University of Wisconsin Milwaukee, Mechanical Engineering Chen, Junhong; University of Wisconsin Milwaukee College of Engineering and Applied Science Lambert, Tristan; Cornell University, Chemistry & Chemical Biology; Columbia University, Chemistry Qu, Deyang; University of Wisconsin Milwaukee College of Engineering and Applied Science, Mechanical Engineering

ARTICLE

A Redox-Active Organic Cation for Safer High Energy Density Li-Ion Batteries

Received 00th January 20xx,
Accepted 00th January 20xx

DOI: 10.1039/x0xx00000x

Weixiao Ji,[‡a] He Huang,[‡b] Xingkang Huang,[a] Xiaoxiao Zhang,[a] Dong Zheng,[a] Tianyao Ding,[a] Junhong Chen,[a] Tristan H. Lambert*[b] and Deyang Qu*[a]

Ni-rich layered cathode materials are at the forefront to be deployed in the high energy density Li-ion batteries for the automotive market. However, the intrinsic poor structural and interfacial stability during overcharging could trigger violent thermal failure, which severely limits their wide application. To protect the Ni-rich cathode from overcharging, we firstly report a redox-active cation, thioether-substituted diaminocyclopropenium, as an electrolyte additive to limit the cell voltage within the safe value during overcharging. The organic cation demonstrates a record-breaking electrochemical reversibility at ~4.55 V versus Li^+/Li and solubility (0.5 M) in carbonate-based electrolyte. The protection capability of the additive was explored in two cell chemistries: a $LiNi_{0.8}Co_{0.15}Al_{0.05}O_2$/graphite cell and a $LiNi_{0.8}Co_{0.15}Al_{0.05}O_2$/silicon-graphene cell with an areal capacity of ~2.2 mAh cm^{-2} and ~3 mAh cm^{-2}, respectively. With 0.2 M addition, the $LiNi_{0.8}Co_{0.15}Al_{0.05}O_2$/graphite cell survived 54 cycles at 0.2 C with 100% overcharge. Moreover, the cell can carry an utmost 4.4 mA cm^{-2} (2 C) with 100% overcharge and a maximum capacity of 7540% SOC at 0.2 C.

1. Introduction

Li-ion batteries (LIBs) are expected to have a cell-level specific capacity of >350 Wh kg^{-1} by 2025 to meet the market demanding driving range of an electric vehicle (EV).[1,2] Among the state-of-the-art cathode materials, Ni-rich layered oxides, $LiNi_xCo_yAl_zO_2$ (NCA) and $LiNi_xCo_yMn_zO_2$ (NCM) with x+y+z=1 and $x \geqq 0.8$, have an unbeatable high capacity of ~200 mAh g^{-1}. Coupled with their relatively low cost due to the low Co content and the high working voltage (3.8 V), the Ni-rich layered cathodes will be at the forefront to boost the energy density of EV batteries.[3-7]

However, the most pressing issue hindering the deployment of Ni-rich cathodes in the EV market is battery safety.[8-10] Due to the intrinsic poor structural stability and high surface activity of Ni-rich materials, severe safety hazards and even a cell thermal runaway can occur under a high potential during an overcharge.[11-14] Over the years, strategies have been investigated to increase cell safety at the material level, such as the surface coating,[15,16] element substitution[17,18] and structural engineering of Ni-rich materials[19-22]. Despite the improvement in thermostability and oxidation-resistance, the complete mitigation of thermal runaway against continued overcharging is still an open challenge.

Besides those strategies, another promising approach is to prevent Ni-rich cathodes from overcharging at the cell level. Reversible overcharge protection can be achieved by adding redox shuttle additives to limit the cell voltage within a safe range.[23] As illustrated in Fig. 1a, during overcharging, the additives can repeatedly undergo oxidation and reduction by shuttling between a cathode and an anode, respectively, acting like a shorted “molecular circuit” to consume the extra electrical energy.[24-27] However, exploiting such redox shuttles for a Ni-rich cathode with the charging cut-off voltage as high as 4.3 V can be extremely challenging and are rarely reported. The main bottleneck is the stability of the shuttles. Due to the open-shell structure, the oxidized molecules have a strong tendency to react with other components in a battery. Those undesired side reactions would lead to a drastic reduction of the protection efficacy. Another obvious issue lies in the poor solubility of the shuttle molecules. Principally, the shuttle molecule concentration dictates the maximum shuttling current. For those reasons, state-of-the-art shuttles devised for 4V-class cathodes (Fig. 1b, not limited to Ni-rich cathodes), mainly derived from the classical structures of dimethoxybenzene[23,28-30] and phenothiazine[31], fall short under practical testing conditions. Arguably, new structural paradigms offer the best opportunity to address these multifaceted challenges.

Recently, we successfully synthesized and deployed a new family of redox shuttle additives, aromatic cyclopropenium salts, for Na-ion batteries under harsh overcharging conditions.[32] The cyclopropenium cation combines the elements of aromaticity and ionicity, leading to superior electrochemical stability and solubility over conventional

[a] Department of Mechanical Engineering, University of Wisconsin Milwaukee, Milwaukee, WI 53211, USA. E-mail: qud@uwm.edu
[b] Department of Chemistry and Chemical Biology, Cornell University, Ithaca, NY 14853, USA. E-mail: Tristan.lambert@cornell.edu
† Electronic Supplementary Information (ESI) available. See DOI: 10.1039/x0xx00000x
‡ These authors contributed equally.

neutral shuttle molecules.[33-36] Together with the other enlightening studies of cyclopropenium

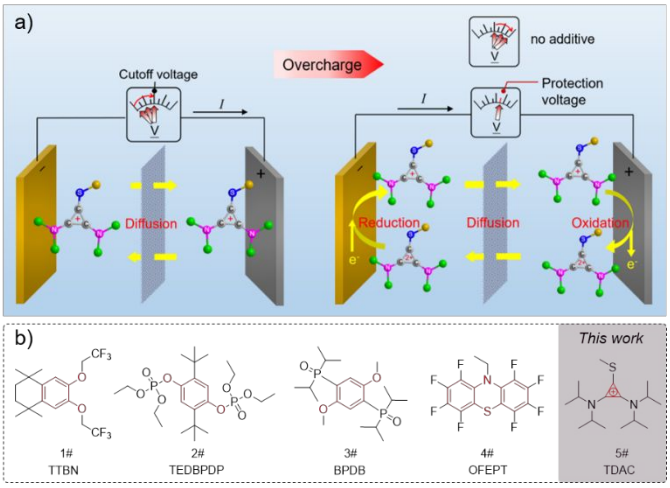

Fig. 1. a) Schematic illustration of the redox shuttle's behavior under cell normal operation and overcharge condition, TDAC molecule was used as an example of redox shuttle; b) chemical structures of state-of-the-art redox shuttles for 4V-class cathodes.

salts in fields such as electrophotocatalysis[37-39] and redox flow batteries[40-43], we envisioned the possibility of devising a high-potential cyclopropenium cation catered to Ni-rich cathodes.

In this contribution, we report the first use of a thioether-substituted diaminocyclopropenium cation (denoted as TDAC) as the redox shuttle for Ni-rich cathodes. The TDAC cation achieved a record-breaking electrochemical reversibility at 4.55 V (versus Li^+/Li) and solubility of 0.5 M in carbonate-based electrolyte. With 0.2 M addition, the $LiNi_{0.8}Co_{0.15}Al_{0.05}O_2$/graphite cell that had an areal capacity of 2.2 mAh cm^{-2} survived 54 cycles at 0.2 C with a 100% overcharge. Meanwhile, the cell carried up to a 4.4 mA cm^{-2} overcharge current and endured an overcharge capacity of 7540% SOC at 0.2 C. The overcharge performance was also explored in a $LiNi_{0.8}Co_{0.15}Al_{0.05}O_2$/silicon-graphene cell with a high areal capacity of 3 mAh cm^{-2}.

2. Experimental

2.1 Synthesis of TDAC•PF_6 compound

Bis-diisopropylaminocyclopropenethione [44] (1.34 g, 5 mmol, 1 equiv) was dissolved in neat dimethyl sulfate (1.0 mL) and the resulting mixture was stirred at 25 °C for 3 h. The reaction was monitored by thin-layer chromatography (TLC). Dichloromethane (25 mL) was added. With vigorous stirring, an aqueous solution of ammonium hexafluorophosphate (1.96 g, 12 mmol in 12 mL of H_2O) was added. A white precipitate formed, and this material was extracted into dichloromethane (3 × 90 mL). The organic extracts were dried over $MgSO_4$ and concentrated under vacuum. The crude product was washed by ethyl acetate and then dried in vacuo. The pure product TDAC was obtained as a white powder (1.39 g, 65% yield).

2.2 Preparation of electrolytes and electrodes

FEC and DMC were purchased from SoulBrain Corp. $LiPF_6$ was purchased from BASF Corp. Li chips (450 μm) were purchased from MTI Corp. The baseline electrolyte is 1 M $LiPF_6$ + DMC/FEC (v/v=8/2). The high fluorine content can provide relatively robust electrolyte/electrode interface toward aggressive chemistries under high potential.[45] The electrolyte used for protection failure study was commercial carbonate electrolyte: 1 M $LiPF_6$ + EC/EMC (v/v=4/6). TDAC•PF_6 crystal powder was dissolved in baseline electrolyte to fabricate 0.2 M TDAC electrolyte. The NCA cathode, LMO cathode and graphite anode were composed of active material, polyvinylidene fluoride (PVDF) binder and Super C carbon at a mass ratio of 90:5:5. The areal capacity of NCA cathode, LMO cathode and graphite anode is 2.2 mAh cm^{-2}. The NCA cathode and silicon-graphene (Si-C) anode sheets, with areal capacity of ~3 mAh cm^{-2}, were friendly provided from Nanograf Corp. The formulation of the anode sheet was Si-C active material (mass ratio of 45:55), PVDF binder and Super C carbon at a mass ratio of 75:5:20. The loading of the NCA cathode and Si-C anode was ~18-19 mg cm^{-2} and ~3-4 mg cm^{-2}, respectively. All electrode sheets were dried under vacuum at 80 °C overnight before use.

2.3 Material Characterization

^1H NMR (500 MHz, Chloroform-d) δ 4.02-3.90 (m, 4H), 2.69 (s, 3H), 1.41 (d, J = 6.8 Hz, 24H). ^{13}C NMR (126 MHz, Chloroform-d) δ 134.1, 104.4, 55.4, 49.9, 21.8, 21.0, 16.7. ^{19}F NMR (470 MHz, Chloroform-d) δ -72.4, -74.0. The viscosity of electrolyte solution was measured via a viscometer (BROOKFIELD DV-II+Pro) at 21 °C. To prepare sample for postmortem study, cells were dissembled in Ar-filled glove box (O_2 and H_2O <0.5ppm) and the as-achieved electrodes were rinsed with DMC solvent three times, and then dried thoroughly. The surface morphology and composition of electrodes were analyzed by field emission scanning electron microscopy (FESEM) using a Hitachi S-4800 microscope equipped with a Bruker Quantax EDS system. The reclaimed electrolyte was analyzed by MS test using AdVion MS (APCI) and NMR.

2.4 Electrochemical measurements

CV measurements were conducted on an electrochemical workstation (CHI660A, USA) with glassy carbon as working electrode (CHI104) and lithium metal as both reference and counter electrode. Fc/Fc^+ redox couple serves as an internal reference (3.2 V vs. Li^+/Li). Standard CR2032 coin cells were assembled inside Ar-filled glovebox with 2035 Celgard separator. 30 μL electrolyte was added to each coin cell with barely no electrolyte spilled out during cell crimping. Galvanostatic charge-discharge studies were conducted on a battery cycler (CT2001D, LAND Electronics Co., China). Before assembling full cells, the Si-C anodes were assembled into half-cells for pre-lithiation, which can reduce the initial irreversible capacity. All cells went through three formation cycles at 0.05 C, 0.1 C and 0.2 C, respectively, until the current drops below 0.05 C.

2.5 Overcharge protection evaluation

For overcharge cycling test, the cells were constantly charging at a certain rate to 200% of their normal capacity (denoted as 100% overcharge) or until a cut-off voltage was reached (4.95 V vs. Li^+/Li), whichever occur first. Then, discharging at the same current rate to normal lower cut-off voltage.

3. Results and discussion

3.1 Physicochemical properties of TDAC cation

We previously reported that the oxidation potential of triamino-substituted cyclopropenium cation was 4.05 V vs Li^+/Li.[32] Because the oxidation potential of the cation can be increased if the electron density of the cyclopropenium cation ring is decreased, a higher redox potential can be achieved by replacing one of the strong π-donating amino groups with a weaker electron donating functional group. A thioether-substituted diaminocyclopropenium cation (TDAC) seems to be a promising candidate.[44,46] To sustain the stability of the radical dication, a methyl group was selected as the sulfur substituent. In contrast to longer aliphatic chains, a methyl group is immune to decomposition by elimination processes.[41] Furthermore, the synthesis can be performed on a multigram scale and without column purification as displayed in Scheme S1.†

As illustrated in Fig. 2a, the TDAC cation possesses a 2π electron aromatic system that can readily undergo a single electron redox reaction to generate the corresponding TDAC radical dication. Fig. 2b presents the redox potential and solubility of TDAC salt in comparison with that of state-of-the-art high-potential shuttle molecules. Ideally, the redox potential (protection potential) should be ~0.2-0.3 V above the upper cut-off voltage of the LIBs (normally at 4.3 V). A lower or higher potential outside the range would have the risk of escalated self-discharge during normal operation or an irreversible decomposition of battery components during overcharging. Additionally, a high solubility is desirable since it determines the maximum shuttling current. In these regards, TDAC outperforms all other shuttle candidates with the adequate redox potential of 4.55 V (vs. Li^+/Li) and the highest solubility of 0.5 M (Fig. S2†). The electrolyte viscosity before and after the TDAC addition was also investigated. The concentration of 0.2 M was found to be the optimal amount. The viscosity of 0.2 M TDAC electrolyte is 2.72 mPa compared with 2.43 mPa of baseline electrolyte. The electro-kinetics of the TDAC cation was next investigated by cyclic voltammetry (CV) analysis as shown in Fig. 2c. Even with the high scan rate of 200 mV s^{-1}, TDAC still exhibited a pair of well-defined redox peaks, implying a fast mass transport process within the bulk electrolyte. As shown in Fig. 2d, the diffusion coefficient of TDAC is determined to be 6×10^{-6} cm^{-2} s^{-1}, which is very comparable with that of other reported shuttles.[24-27] As displayed in Fig. 2e, after 1000 CV scans, the potential gap between the anodic and cathodic peaks becomes only 60 mV wider, and there is no obvious deterioration of the peak current intensity. Such excellent electrochemical stability has rarely been reported among other 4V-class shuttles.[23,28-31] The inset photograph in Fig. 2e presents a shiny Li surface with no bubble generation after storing in TDAC-containing electrolyte solution for six months, indicating a high chemical inertness of TDAC cation toward Li metal.

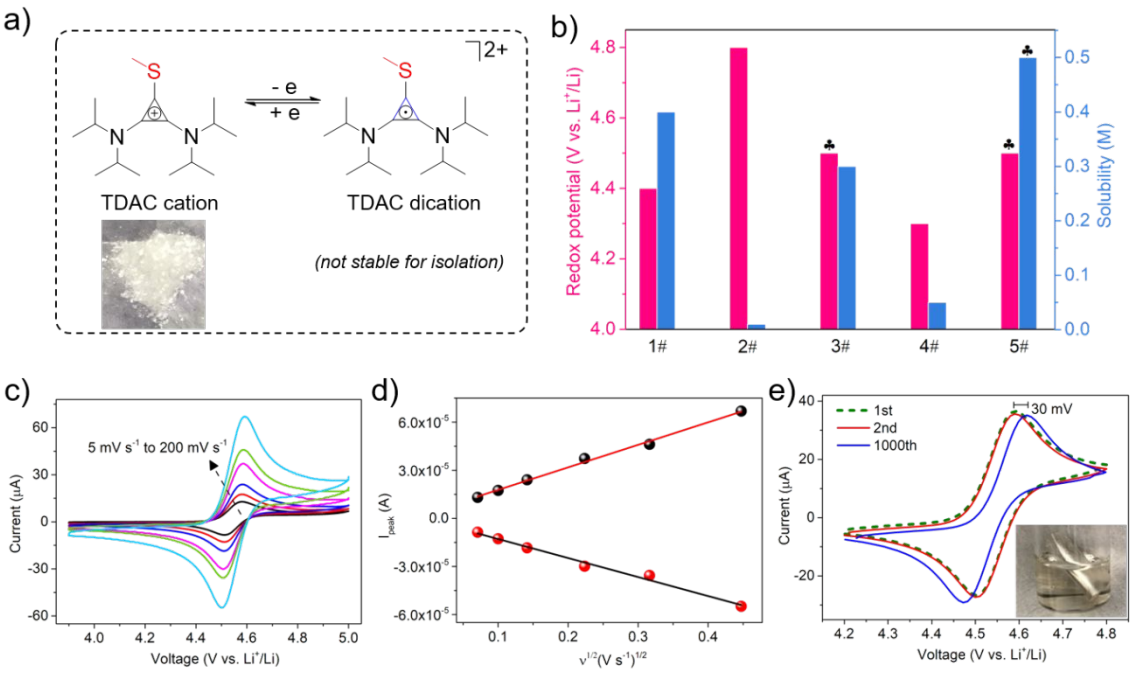

Fig. 2. a) Electrochemical conversion of TDAC redox pairs and a photograph of TDAC•PF_6 salt; b) comparison of redox potential and solubility of state-of-the-art high-potential shuttles; c) cyclic voltammograms at various scan rates; d) plots of peak current vs square root of scan rate and linear fits; e) cyclic voltammograms scanned at 100 mV s^{-1} and a photograph of Li disk stored in 20 mM TDAC electrolyte after six months.

3.2 Overcharge performance of LIBs with 0.2 M TDAC electrolyte

To study the protection of TDAC on Ni-rich cathodes, $LiNi_{0.8}Co_{0.15}Al_{0.05}O_2$ (NCA) was selected as the cathode while graphite and silicon-graphene (Si-C) composite were applied as the anodes. NCA/graphite cells and NCA/Si-C cells were fabricated at a loading of 2.2 mAh cm^{-2} and 3 mAh cm^{-2}, respectively. Compared with the Ni-rich low Co NCM cathodes, NCA possesses a better chemical and electrochemical stability and rate capability due to the existence of Al. For example, the EV batteries with the NCA cathodes for Tesla Model S deliver a long driving range of 595 km.[2] As the next-generation anode, the silicon-based alloys are especially appealing with their high gravimetric capacity (~4200 mAh g^{-1}) and cost-effectiveness.[47-49]

As illustrated in Fig. 3a, the oxidation peak of the TDAC cation appears 250 mV after the completion of the delithiation process of NCA, while the reduction peak of the TDAC radical dication appears 200 mV before the start of the lithiation process of NCA. Clearly, the TDAC cation can stay electro-inactive during the normal discharge and recharge of the cell. As shown in Fig. 3b, the NCA/graphite cell displays the protection voltage plateau at ~4.5 V and the cell discharge voltage plateau at ~3.72 V. In comparison with NCA/Li and graphite/Li half-cell data, also shown in Fig. 3b, no polarization is evident. The overcharge protection ability under the high charging rates was also evaluated since an overcharge is more likely to occur at the end of a fast charging process in real-world scenarios.[50,51] As displayed in Fig. 3c, the NCA/graphite cell can sustain an utmost 2 C charging rate with a 100% overcharge before reaching 4.95 V. The TDAC outperformed the U.S. Advanced Battery Consortium (USABC) fast charging standard, which required that the total battery capacity reach 40% with a 15 min charge (~1.6 C).[52] As shown in Fig. 3d, the NCA/graphite cell can sustain ~377 h (equal to 7540 % SOC) at 0.2 C before reaching 4.95 V. The voltage fluctuation above 4.7 V may be attributed to possible side reactions, e.g. gas evolution.

Finally, the protection reversibility was investigated by cycling the cell at 0.2 C. As shown in Fig. 3e, the TDAC provides the overcharge protection to the NCA/graphite cell for 54 cycles (~750 h) of 100% overcharge. Similar levels of protection were also shown in the NCA/Si-C cell with a 1.5 times higher areal capacity than that of the NCA/graphite cell. As shown in Fig. S3a-b,† the NCA/Si-C cell can carry an utmost 3 mA cm^{-2} current (1 C) with 100% overcharge and endure ~355 h (equal to 7100% SOC) at 0.2 C. As exhibited in Fig. S3c,† the NCA/Si-C cell survived 29 cycles with 100% overcharge at 0.2 C. Other commercial cathode materials like NCM111, $LiMn_2O_4$ and $LiCoO_2$, were also tested in 0.2 M TDAC electrolyte (Fig. S4-5†). The results prove that TDAC is a universal electrolyte additive design for 4V-class cathodes' overcharge protection. Besides, TDAC exhibit a relatively low manufacturing cost of $5.8 per gram (Fig. S6†).

The performance summary of the state-of-the-art shuttle molecules for 4V-class cathodes is tabulated in Table S1.† However, none of the previous studies could simulate the overcharge conditions for a commercial LIB. The tests reported in the literature were either in a half-cell or with a low areal capacity (<2 mAh cm^{-2}) or at a low testing rate (0.1 C). In contrast, our study exhibited the best overcharge protection performance ever reported. The protection current (4.4 mA cm^{-2}), capacity (7540 % SOC) and reversibility (54 cycles) were demonstrated.

3.3 Electrochemical performance of LIBs during normal operation

Understanding the impact of a shuttle additive on the battery's normal operation is very critical before its practical implementation. The rate performance of the NCA/graphite cell between 2.8-4.3 V was evaluated and the results are shown in Fig. 4a. The capacity retention of the cells with the baseline electrolyte and the TDAC containing electrolyte was 98% vs. 98% at 0.2 C, 94.5% vs. 94% at 0.5 C, 89% vs. 87% at 1 C and 80% vs. 74% at 2 C, respectively. The performance was similar between the two electrolytes except under 2 C, in which the sluggish Li^+ transport in the more viscous TDAC electrolyte may play a role. Fig. 4b shows that the NCA/graphite cell with TDAC containing electrolyte remains at 78.1% capacity with a nearly 100% Coulombic efficiency (CE) after 450 cycles at 0.5 C. As shown in Fig. S7,† the NCA/Si-C cell with TDAC containing electrolyte remains at 88.3% capacity with a nearly 100% CE after 200 cycles at 0.5 C. Overall, the TDAC cation did not exert any obvious adverse effect on the performance of the LIBs against that of the baseline electrolyte.

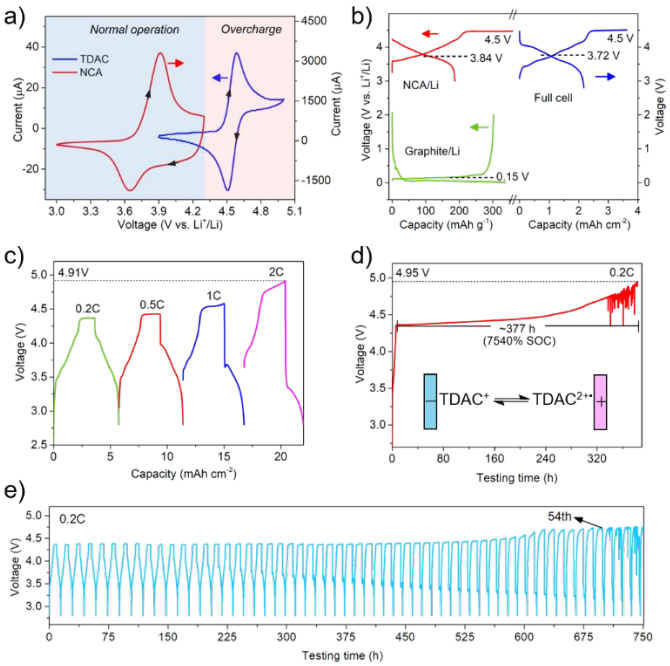

Fig. 3. a) Comparison of cyclic voltammograms between TDAC cation and NCA cathode; b) voltage profiles of NCA/graphite full cell, NCA/Li half-cell and graphite/Li half-cell, respectively; c) 100% overcharge profiles at different current rates; d) continuously charging voltage profile at 0.2 C; e) 100% overcharge cycling performance at 0.2 C.

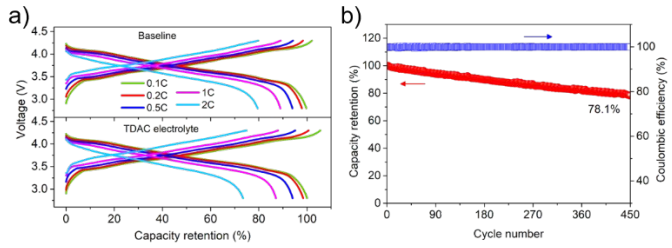

Fig. 4. a) Rate performance and b) 0.5 C cycling performance of NCA/graphite cell between 2.8-4.3 V.

3.4 Post-mortem study on the mechanism of protection failure

To investigate the failure mechanism of the overcharge protection of the TDAC, a scaled-up NCA/graphite cell was employed to reclaim enough electrolyte and electrode materials for a post-mortem analysis. The reclaimed electrolyte after overcharge was a brownish color, which could be attributed by the dissolution of the transition metals (Co, Ni) from the cathode, the decomposition products of the electrolyte solvent, or the TDAC molecules under the harsh overcharge environment. MS, NMR and CV were used to analyse the reclaimed electrolyte in comparison with the fresh electrolyte. Fig. 5a shows a peak at a 283.2 mass/charge ratio (m/z) for both electrolytes. The MS data confirmed the existence of TDAC cation species in both electrolytes. The similar intensity of the peaks indicated that the concentration of the TDAC in the overcharged electrolyte was about the same as that in the fresh one. NMR analysis in Fig. 5b also confirmed that most of the TDAC remained intact since no TDAC decomposed compounds were detected. The CV profile in Fig. 5c reveals a pair of reversible redox peaks at ~1.35 V vs. Fc^+/Fc, exhibiting no discrepancy against the fresh TDAC electrolyte. The reclaimed electrolyte was then injected into a cell with new NCA and graphite sheets. As displayed in Fig. 5d, the potential plateau at ~4.5 V reappeared in the reassembled cell despite a lower CE and a decreased capacity.

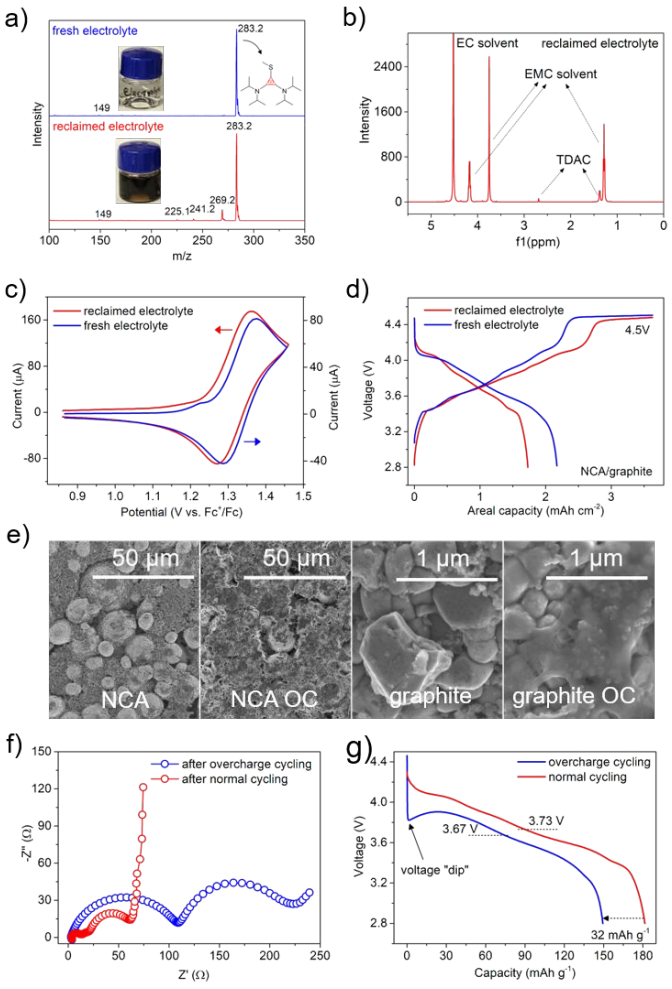

Fig. 5. a) Mass spectrum and photographs of different electrolytes; b) NMR spectra of the reclaimed electrolyte; c) cyclic voltammetry profiles; d) overcharge profiles of NCA/graphite cell; e) SEM images of reclaimed electrodes compared with electrodes cycled within normal voltage range after 50 cycles; f) EIS spectra and g) discharge profiles of NCA/graphite cells.

The reclaimed electrodes were then analysed by SEM and EDS mapping. As shown in Fig. 5e, thick films were observed on both the reclaimed cathode and the anode. The surfaces of the NCA cathode and the graphite anode are more defined after normal cell operation. Ni, Co, S and N element can be observed on the reclaimed graphite sheet from the EDS mapping shown in Fig. S9-10.† It was reported that upon overcharging, unstable Ni^{4+} could be generated and tended to react with the electrolyte, forming a thick interface on the cathode. Meanwhile, these ions can also migrate to the graphite anode and get reduced there.[53] The poisoned anodes could further catalyse the electrolyte decomposition and cause the formation of an even thicker film on the anode. The substantial increase of the cell impedance is reflected in Fig. 5f. The charge transfer reactions at the interface could be affected as well. The charge transfer reactions included both the delithiation and lithiation reaction of active materials, and the redox reaction of TDAC molecules. As displayed in Fig. 3e and Fig. 5g, the voltage hysteresis was gradually increased in the discharge profiles upon overcharge cycling. In addition, a "voltage dip" appeared at the initial stage of the discharge process, indicating the IR drop.[54,55] Therefore, the main reason of the protection failure was that the charge transfer at the electrolyte/electrode interface was blocked by the thick surface film formed during the overcharge. Moreover, the less soluble radical dication could be precipitated on the electrode surface, which would further deteriorate the TDAC ability of overcharge protection. Again, these findings emphasized the importance of the anodic stability of electrolyte, the interfacial stability of cathode material and the solubility of redox shuttle additive for a better overcharge protection performance.

Conclusions

In summary, this study exploited a thiomethyl-substituted cyclopropenium cation (TDAC) as the overcharge protection additive for Ni-rich cathodes. TDAC cation exhibits an unmatched electrochemical stability and solubility. With 0.2 M TDAC addition, the NCA/graphite cell survived 54 cycles at 0.44

mA cm^{-2} with 100% overcharge and can carry up to 4.4 mA cm^{-2} overcharge current. This work clears the long-existing obstacles of developing high-potential redox shuttles for 4V-class Ni-rich cathodes' overcharge protection.

Conflicts of interest

There are no conflicts to declare.

Acknowledgements

This material is based upon work supported by the U.S. Department of Energy's Office of Energy Efficiency and Renewable Energy (EERE) under the National Energy Technology Lab Award Number DE-EE0008859 (D.Y.Q) and Cornell University.

Notes and references

1 M. Li, J. Lu, Z. Chen, K. Amine, *Adv. Mater*. 2018, **30**, 1800561.
2 W. Li, E. M. Erickson, A. Manthiram, *Nature Energy* 2020, **5**, 26-24.
3 J. Kim, H. Lee, H. Cha, M. Yoon, M. Park, J. Cho, *Adv. Energy Mater.* 2018, **8**, 1702028.
4 A. Manthiram, *Nature Comm.* 2020, **11**, 1-9.
5 S. S. Zhang, *Energy Storage Mater.* 2020, **24**, 247-254.
6 X. Wang, Y. L. Ding, Y. P. Deng, Z. Chen. *Adv. Energy Mater.* 2020,**10**, 1903864.
7 S. S. Zhang, *J. Energy Chem.* 2020, **41**, 135-141.
8 X. Feng, M. Ouyang, X. Liu, L. Lu, Y. Xia, X. He, *Energy Storage Mater.* 2018, **10**, 246-267.
9 X. Liu, D. Ren, H. Hsu, X. Feng, G. L. Xu, M. Zhuang, H. Gao, L. Lu, X. Han, Z. Chu, J. Li, X. He, K. Amine, M. Ouyang, *Joule* 2018, **2**, 2047-2064.
10 K. Liu, Y. Liu, D. Lin, A. Pei, Y. Cui, *Sci. Adv.* 2018, **4**, eaas9820.
11 X. Zhu, Z. Wang, Y. Wang, H. Wang, C. Wang, L. Tong, M. Y, *Energy* 2019, **169**, 868-880.
12 K. W. Nam, S. M. Bak, E. Hu, X. Yu, Y. Zhou, X. Wang, L. Wu, Y. Zhu, K. Y. Chung, X. Q. Yang, *Adv. Funct. Mater.* 2013, **23**, 1047-1063.
13 D. Belov, M. H. Yang. *J. Solid State Electrochem.* 2008, **12**, 885-894.
14 D. Ren, X. Feng, L. Lu, M. Ouyang, S. Zheng, J. Li, X. He, *J. Power Sources*, 2017, **364**, 328-340.
15 S. U. Woo, C. S. Yoon, K. Amine, I. Belharouak, Y. K. Sun, *J. Electrochem. Soc.* 2007, **154**, A1005-A1009.
16 M. L. Zhang, H. Y. Zhao, M. Tan, J. T. Liu, Y. Z. Hu, S. S. Liu, X. H. Shu, H. Li, Q. W. Ran, J. J. Cai, X. Q. Liu, *J. Alloys Compd.* 2019, **774**, 82-92.
17 S. U. Woo, B. C. Park, C. S. Yoon, S. T. Myung, J. Prakash, Y. K. Sun, *J. Electrochem. Soc.* 2007, **154**, A649-A655.
18 W. Cho, Y. J. Lim, S. M. Lee, J. H. Kim, J. H. Song, J. S. Yu, Y. J. Kim, M. R. Park, *ACS Appl. Mater. Interfaces* 2018, **10**, 38915-38921.
19 Y. K. Sun, D. H. Kim, H. G. Jung, S. T. Myung, K. Amine, *Electrochim. Acta* 2010, **55**, 8621-8627.
20 J. Y. Liao, A. Manthiram, *J. Power Sources* 2015, **282**, 429-436.
21 P. Y. Hou, X. Q. Wang, D. W. Song, X. X. Shi, L. Q. Zhang, J. Guo, J. Zhang, *J. Power Sources* 2014, **265**, 174-181.
22 Y. K. Sun, B. R. Lee, H. J. Noh, H. M. Wu, S. T. Myung, K. Amine, *J. Mater. Chem.* 2011, **21**, 10108-10112.
23 W. Weng, J. Huang, I. A. Shkrob, L. Zhang, Z. Zhang, *Adv. Energy Mater.* 2016, **6**, 1600795.
24 Z. Chen, Y. Qin, K. Amine, *Electrochim. Acta* 2009, **54**, 5605-5613.
25 C. Buhrmester, L. Moshurchak, R. L. Wang, J. R. Dahn, *J. Electrochem. Soc.* 2006, **153**, A288-A294.
26 J. R. Dahn, J. Jiang, L. M. Moshurchak, M. D. Fleischauer, C. Buhrmester, L. J. Krause, *J. Electrochem. Soc.* 2005, **152**, A1283-A1289.
27 L. M. Moshurchak, C. Buhrmester, J. R. Dahn, *J. Electrochem. Soc.* 2008, **155**, A129-A131.
28 L. Zhang, Z. Zhang, H. Wu, K. Amine, *Energy & Environ. Sci.* 2011, **4**, 2858-2862.
29 J. Huang, N. Azimi, L. Cheng, I. A. Shkrob, Z. Xue, J. Zhang, N. L. Dietz Rago, L. A. Curtiss, K. Amine, Z. Zhang, L. Zhang, *J. Mater. Chem. A* 2015, **3**, 10710-10714.
30 L. M. Moshurchak, W. M. Lamanna, M. Bulinski, R. L. Wang, R. R. Garsuch, J. Jiang, D. Magnuson, M. Triemert, J. R. Dahn, *J. Electrochem. Soc.* 2009, **156**, A309-A312.
31 A. P. Kaur, M. D. Casselman, C. F. Elliott, S. R. Parkin, C. Risko, S. A. Odom, *J. Mater. Chem. A* 2016, **4**, 5410-5414.
32 W. Ji, H. Huang, X. Zhang, D. Zheng, T. Ding, T. H. Lambert, D. Qu, *Nano Energy* 2020, **72**, 104705.
33 J. S. Bandar, T. H. Lambert, *Synthesis* 2013, **45**, 2485-2498.
34 R. W. Johnson, *Tetrahedron Lett.* 1976, **17**, 589-592.
35 R. Weiss, K. Schloter, *Tetrahedron Lett.* 1975, **16**, 3491-3494.
36 F. Gerson, G. Plattner, Z. Yoshida, *Mol. Phys.* 1971, **21**, 1027-1032.
37 H. Huang, Z. M. Strater, M. Rauch, J. Shee, T. J. Sisto, C. Nuckolls, T. H. Lambert, *Angew. Chem. Int. Ed.* 2019, **58**, 13318-13322.
38 H. Huang, T. H. Lambert, *Angew. Chem. Int. Ed.* 2020, **59**, 658-662.
39 H. Huang, Z. M. Strater, T. H. Lambert, *J. Am. Chem. Soc.* 2020, **142**, 1698-1703.
40 C. S. Sevov, S. K. Samaroo, M. S. Sanford, *Adv. Energy Mater.* 2017, **7**, 1602027.
41 Y. Yan, S. G. Robinson, M. S. Sigman, M. S. Sanford, *J. Am. Chem. Soc.* 2019, **141**, 15301-15306
42 K. H. Hendriks, S. G. Robinson, M. N. Braten, C. S. Sevov, B. A. Helms, M. S. Sigman, S. D. Minteer, M. S. Sanford, *ACS Cent. Sci.* 2018, **4**, 189-196.
43 S. G. Robinson, Y. Yan, K. H. Hendriks, M. S. Sanford, M. S. Sigman, *J. Am. Chem. Soc.* 2019, **141**, 10171-10176.
44 Z. Yoshida, H. Konishi, H. Ogoshi, *Isr. J. Chem.* 1981, **21**, 139-144.
45 X. Fan, L. Chen, O. Borodin, X. Ji, J. Chen, S. Hou, T. Deng, J. Zheng, C. Yang, S.-C. Liou, K. Amine, K. Xu, C. Wang, *Nat. Nanotech.* 2018, **13**, 715-722.
46 K. Komatsu, T. Kitagawa, *Chem. Rev.* 2003, **103**, 1371-1428.
47 P. Li, G. Zhao, X. Zheng, X. Xu, C. Yao, W. Sun, S. X. Dou, *Energy Storage Mater.* 2018, **15**, 422-446.
48 K. Feng, M. Li, W. Liu, A. G. Kashkooli, X. Xiao, M. Cai, Z. Chen, *Small* 2018, **14**, 1702737.
49 S. Chae, M. Ko, K. Kim, K. Ahn, J. Cho, *Joule* 2017, **1**, 47-60.
50 J. Lopez, M. Gonzalez, J. C. Viera, C. Blanco, *IEEE* 2004, 19.
51 Y. Liu, Y. Zhu, Y. Cui, *Nature Energy* 2019, **4**, 540-550.
52 USABC Electric Vehicle Battery Test Procedures Manual. Revision2, https://digital.library.unt.edu/ark:/67531/metadc666152/(accessed: January 1996).
53 Y. Li, X. Liu, D. Ren, H. Hsu, G. Xu, J. Hou, L. Wang, X. Feng, L. Lu, W. Xu, Y. Ren, R. Li, X. He, K. Amine, M. Ouyang, *Nano Energy* 2020, **71**, 104643.
54 D. Qu, *J. Power Sources* 2006, **162**, 706-712.
55 D. Qu, *Electrochem. Comm.* 2006, **8**, 1527-1530.

